Design of Compact Dual-Polarized Printed-Circuit Antenna for Ultra-Wideband Applications

K. Rambabu, M.Z. Alam and J. Bornemann*

Department of Electrical and Computer Engineering
University of Victoria, Victoria, BC, Canada V8W 3P6

Abstract — **This paper presents a small printed-circuit antenna, which is well suited for ultra-wideband and dual-polarized applications. By exciting six fundamental-mode resonance frequencies and utilizing their respective harmonics, a broadband operation is achieved covering a frequency range between 4.6 and 13.6 GHz with a VSWR less than 2.2 and a gain better than 2 dBi. The design is verified by commercially available software and measurements.**

Index Terms — **Ultra-wideband antennas, printed-circuit antennas, multi-resonance antennas.**

I. Introduction

Ultra-wideband (UWB) or pulsed (time-domain) communication is becoming increasingly popular for short-range and high bandwidth applications, e.g. [1]. UWB antenna performance can be achieved with traditional antenna configurations like the log periodic form or the zigzag approach, e.g. [2]. In order to achieve antenna miniaturization for handset applications, it is necessary to employ printed-circuit technology on a relatively small substrate area. Such compact wideband dual-polarized patch antennas have been proposed in [3], [4]. By overlapping three squared patches along their diagonals, the bandwidth can be significantly increased.

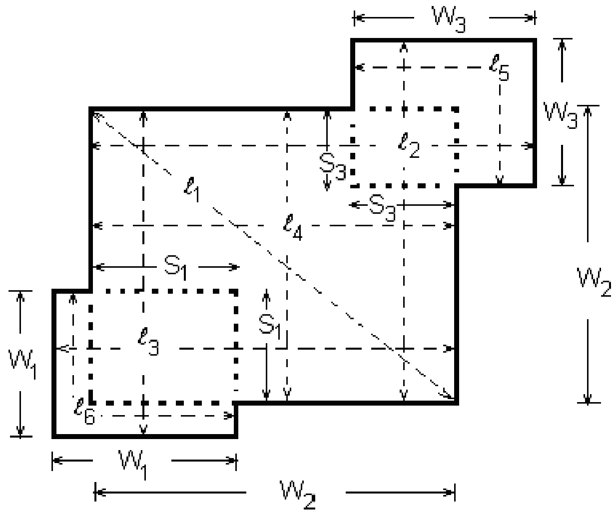

Fig. 1. Basic layout of the compact dual-polarized printed-circuit antenna for UWB applications.

Since in wireless communications, polarization loss is encountered due to random scattering from objects and obstructions in urban environments, dual-polarized antennas offer an advantage over devices operating, e.g., in a single linear polarization.

This paper focuses on the principle design strategies for the patch antenna with overlapping squares (Fig. 1) in order to present the design engineer with guidelines and achievable performance characteristics.

II. Design

This section presents the design by overlapping patches and explains the basic design philosophy.

A. Design Principle

The design principle is based on staggering different patches (resonators) and combining them in a single metallization on a substrate as shown in Fig. 1. The different resonant frequencies must be separated such that the overall integration of the resonant frequencies will result in satisfactory UWB performance. The achievable bandwidth depends on the number of resonances.

As is indicated in Fig. 1, the proposed radiating structure has six different physical dimensions related to different basic resonances. The first (f_1) and sixth (f_6) resonant frequencies should be chosen such that the harmonic of the first basic resonance ($f_7 = 2f_1$) will be able to integrate with f_6. Similarly, the harmonics of f_2 to f_6 form resonances at f_8 to f_{12} and extend the bandwidth towards higher frequencies. By covering the lower part of the bandwidth with basic resonances and the upper part with harmonics, it is possible to stagger twelve resonances, thus achieving a UWB performance.

B. Design Method

This section presents the design steps to achieve six different basic resonant frequencies, which are closely spaced to yield wide bandwidth.

Step 1: Chose the dimensions ($W_2 \times W_2$) of the center square patch such that the fourth basic resonance (f_4) will be approximately at the

* K. Rambabu and M.Z. Alam were with the University of Victoria, Victoria, BC, V8W 3P6, Canada. K. Rambabu is now with the Institute for Infocomm Research, Singapore 117674; M.Z. Alam is now with the University of Toronto, ON, M5S 3G4, Canada.

center of the lower half of the desired band.

Step 2: Chose the dimensions ($W_1 \times W_1$) and S_1 such that f_4 and f_3 integrate as a single band.

Step 3: Chose the dimensions ($W_3 \times W_3$) and S_3 such that f_2 can be integrated into already developed bandwidth due to f_4 and f_3.

Step 4: Chose W_3 and S_3 such that f_5 will be included and improves the existing bandwidth. From step 3 and step 4 the values for W_3 and S_3 can be estimated.

Step 5: Chose W_1 and S_1 such that f_6 will add to the bandwidth. The values for W_1 and S_1 can be estimated from step 4 and step 5.

By proper feeding (see below) it is possible to excite the diagonal mode with resonant frequency f_1 together with f_2 to f_6 and their individual harmonics.

The physical dimensions of the patch are related to the resonant lengths by the following set of equations, which provide the design engineer with very good first-order design guidelines.

$$\begin{aligned} l_1 &= \sqrt{2}W_2 + 2\Delta l_1 \\ l_2 &= W_2 + (W_3 - S_3) + 2\Delta l_2 \\ l_3 &= W_2 + (W_1 - S_1) + 2\Delta l_3 \\ l_4 &= W_2 + 2\Delta l_4 \\ l_5 &= 2W_3 - (W_3 - S_3) + 2\Delta l_5 \\ l_6 &= 2W_1 - (W_1 - S_1) + 2\Delta l_6 \end{aligned} \quad (1)$$

The excess lengths Δl_1, Δl_2, Δl_3, Δl_4, Δl_5, Δl_6 correspond to the fringing fields created by line widths l_1, l_2, l_3, l_4, l_5, l_6, respectively. They can be straightforwardly determined from [5].

C. Feeding Technique

In principle, this structure can be probe fed. However, the probe inductance will limit the achievable bandwidth. Therefore, a capacitive pad is provided, as shown in Fig. 2, to compensate for the probe reactance at higher frequencies.

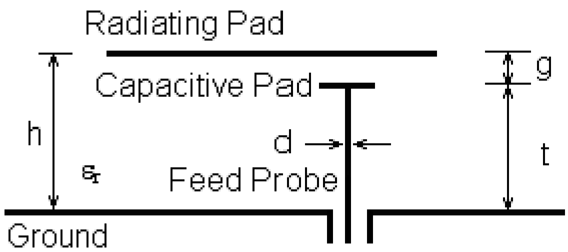

Fig. 2. Feeding mechanism of UWB printed-circuit antenna.

The probe inductance, L, and pad capacitance, C, can be estimated by the following empirical equations

$$L = \frac{\mu_0}{2\pi} t \left[\ln\left(\frac{4t}{d}\right) + 0.5\left(\frac{d}{t}\right) - 0.75 \right] \quad (2)$$

$$C = \frac{\varepsilon_r \varepsilon_0 (x + \Delta p)(y + \Delta p)}{g}, \quad \Delta p = \frac{4g \ln(2)}{\pi} \quad (3)$$

where x and y are the dimensions of the capacitive pad, and all other quantities are according to Fig. 2. More generalized formulations can be found in [6]. To select a feed location for better performance, S_1 and S_2 in Fig. 1 can be optimized using full wave commercial software.

D. Radiation Characteristics

At each resonant frequency, the overlapping-squares antenna has vertical and horizontal radiating edges, which will radiate to give dual-polarized radiation. Even though the radiated field has uniform vertical and horizontal components, due to the lack of proper phase difference between them, purely circular polarization is hardly possible over a wide frequency range. However, at particular frequency points, nearly circular polarization might occur.

The orientation of the main beam at a particular frequency depends on the excitation levels of the vertically and horizontally radiating edges. Due to uneven excitation of these field components, the main beam may tilt towards the stronger excitation. The antenna gain may decrease at the band edges due to the small radiating aperture compared to conventional microstrip patch antennas.

III. Results

To demonstrate the above theory and present typical performance characteristics, a UWB antenna on a substrate with ε_r=2.35 and thickness h=3.42 mm was designed. The dimensions of the three square patches and their overlapping sides are W_1=7.5 mm, W_2=13.5 mm, W_3=9.5 mm, S_1=6.5 mm and S_3=7 mm. The gap between the radiating patch and the feed is g=0.25 mm, and the dimensions of the capacitive pad are 2.5×2.5 mm^2.

Although it is known that thicker substrates give better bandwidth, the height of this substrate of h=3.42 mm (including two layers of 3.17 mm and 0.25mm) is relatively small as compared to other designs reported in the literature.

The feed point in Fig. 1 with respect to the lower left corner of the entire structure is located at 3.25 mm to the right and 9.5 mm up. By choosing the optimal feed point it is possible to excite the diagonal mode corresponding to the shorter diagonal so that six different resonant lengths (ℓ_1 to ℓ_6 in Fig. 1) are obtained on the antenna. A disadvantage of the probe feed is that at higher frequencies, the probe inductance tends to limit the bandwidth of the antenna. However, the capacitive pad can be designed such that it partly compensates for this effect.

In order to demonstrate the effect of the overlapping patches with respect to the fundamental and harmonic resonances, the real and imaginary parts of the input impedance of the antenna – as computed with Ansoft Designer® - are shown in Fig. 3. In the lower frequency range, resonances are noted at frequency points, where the imaginary part is zero and the real part is either maximum or minimum. At higher frequencies, the probe inductance dominates the capacitance introduced by the compensating pad by approximately 20 ohms (as indicated by the ellipse in Fig. 3).

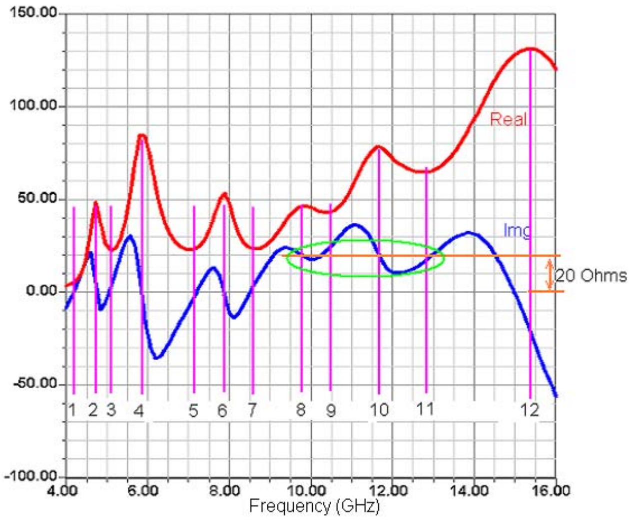

Fig. 3. Real and imaginary part of the input impedance of the UWB antenna (Ansoft Designer®).

In a design scenario, the fundamental resonances and their harmonics are determined from the design expressions given in (1) which include the effects of fringing fields. Table I shows a comparison between such theoretical resonances and those obtained by the commercial software package Ansoft Designer®. Considering the simplicity of the model using only path lengths and fringing lengths, very good agreement is observed.

TABLE I
Resonance frequencies of individual antenna paths; comparison of theory (1) with Ansoft Designer®.

Resonant length (c.f. Fig. 1)	Resonant frequency using (1)	Resonant frequency using Ansoft Designer
Main diagonal	3.68	Not excited
Diagonal ℓ_1	4.44	4.18
Side ℓ_2	4.93	4.74
Side ℓ_3	5.41	4.96
Side ℓ_4	5.79	5.79
Curve ℓ_5	6.97	7.12
Curve ℓ_6	8.03	7.85
Harmonic of ℓ_1	8.88	8.50
Harmonic of ℓ_2	9.86	9.77
Harmonic of ℓ_3	10.82	10.45
Harmonic of ℓ_4	11.59	11.61
Harmonic of ℓ_5	13.94	12.76
Harmonic of ℓ_6	16.06	15.33

As mentioned earlier, the orientation and overlap of the patches and their resulting resonant paths form two perpendicular resonance directions at every resonant frequency, thus facilitating dual-polarized radiation. As an example, the radiation patterns in the two perpendicular planes at 6 GHz are shown in Fig. 4. An analysis of the axial ratio versus frequency (Fig. 5) indicates that nearly circular polarization occurs in only three narrow frequency bands at which the phase difference of the two perpendicular field components is in the vicinity of 90 degrees. However, even in these bands, the axial ratio does not drop below 3dB. Thus for the vast majority of frequencies in the wide spectrum between 4GHz and 16GHz, the antenna radiation is dual-polarized rather than circularly polarized.

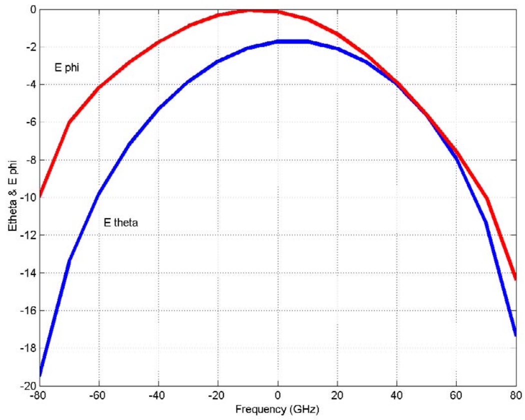

Fig. 4. Radiation patterns of E_θ and E_ϕ in dB at 6 GHz.

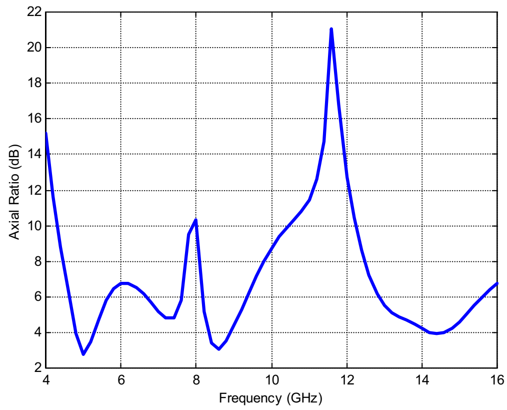

Fig. 5. Axial ratio in dB, demonstrating dual polarization.

The gain of the antenna is shown in Fig. 6. It remains above 2 dBi between 4.6 GHz and 13.6 GHz and decreases towards higher frequencies. Note that this gain plot is for the plane $\theta = 30^0$ and $\phi = 45^0$. It was found that due to the unequal excitation of the perpendicular polarizations at each resonant frequency, the main beam is squinted towards that direction at higher frequencies.

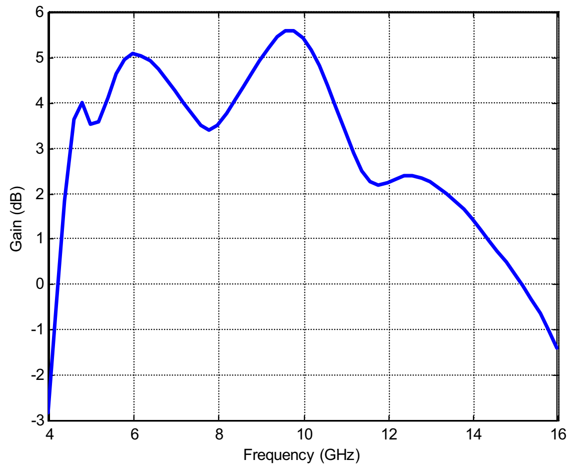

Fig. 6. Gain performance of UWB antenna.

Gain variation with frequency is a known fact in UWB antennas. Especially in this design, the gain variation occurs due to the unequal radiation aperture sizes at different frequencies. For a comparison of performance characteristics of a large number of UWB antennas, the reader is referred to [4].

Fig. 7 shows the input VSWR computed with both Ansoft Designer® and HFSS®. Very good agreement is obtained, hence confirming the UWB character of the performance. Between the 2-dBi-gain frequencies, the computed VSWR is better than 2.2.

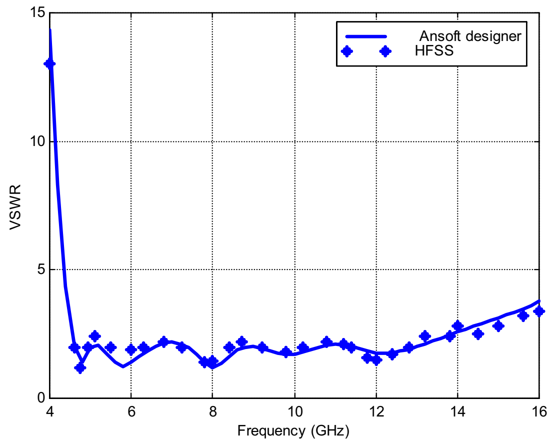

Fig. 7. Wideband VSWR performance evaluated with Ansoft Designer® and HFSS®.

In order to verify the principle design strategy, a prototype was fabricated and its VSWR measured over frequency. However, since a dielectric sheet with ε_r=2.35 and 0.25mm thickness was unavailable at the time of fabrication (c.f. Section III, first paragraph), a thickness of 0.8mm was chosen and this modified design slightly optimized for better bandwidth using Ansoft Designer®. Fig. 8 shows the comparison between measured and simulated VSWR's of the antenna. The VSWR is less then 2.2 for a bandwidth of about 99 percent.

VI. Conclusion

Principle design guidelines for a compact dual-polarized printed-circuit antenna for UWB applications are presented. The wideband performance is obtained through the excitation of a multitude of fundamental resonances and their individual harmonic frequencies. Since each resonance is excited in two polarizations, the radiation characteristics support dual-polarization operation. The prototype design example features a 99 percent bandwidth in which the gain is better than 2 dB and the VSWR better than 2.2.

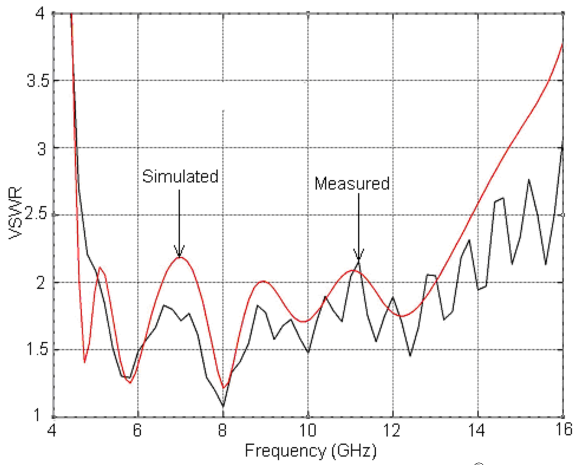

Fig. 8. Measured and simulated (Ansoft Designer®) VSWR of the UWB antenna prototype.

References

[1] B. Pattan, "A brief exposure to ultra-wideband signaling", Microwave J., Vol. 46, pp. 104-110, Dec. 2003.

[2] S.K. Sharma and L. Shafai " Investigations on miniaturized endfire vertically polarized quasi-fractal log-periodic ZigZag antenna", IEEE Trans. Antennas Propagat., Vol. 52 , pp.1957-1962, Aug 2004

[3] K. Rambabu, M. Alam, J. Bornemann and M.A. Stuchly, "Compact wideband dual-polarized microstrip patch antenna", in 2004 IEEE AP-S Int. Symp Dig., pp. 1955-1958, Monterey, USA, June 2004, Monterey, USA, June 2004.

[4] M.Z. Alam and M.A. Stuchly, "Multiresonance planar patch antenna", Microwave Opt. Tech. Lett., pp. 99-103, Vol. 46, July 2005.

[5] K.C. Gupta, R. Garg, I. Bahl and P. Bhartia, Microstrip Lines and Slotlines, pp. 180-183, 2nd ed., Boston: Artech House, 1996.

[6] B.C. Wadell, Transmission-Line Design Handbook, Artech House, Boston, 1991.